Paper:

Machining Performance of Robot-Type Machine Tool Consisted of Parallel and Serial Links Based on Calibration of Kinematics Parameters

Keisuke Nagao, Nobuaki Fujiki, Hiroto Tanaka, Akio Hayashi, Hidetaka Yamaoka, and Yoshitaka Morimoto†

Kanazawa Institute of Technology
7-1 Ohgigaoka, Nonoichi, Ishikawa 921-8501, Japan
†Corresponding author, E-mail: mosandb1@neptune.kanazawa-it.ac.jp
[Received February 16, 2021; accepted April 20, 2021]

This study aims to calibrate the posture of a robot-type machine tool comprising parallel and serial links using a kinematics error model and verify the machining performance based on the measurement results of a machined workpiece calibrated with kinematics parameters. A robot-type machine tool (XMINI, Exechon Enterprises LLC) is used in this study. Typically, the performance required of a robot-type machine tool is not only dimensional accuracy but also the contour accuracy of the machined workpiece. Therefore, in this study, we first construct a forward kinematics model of a robot-type machine tool and identify the kinematics parameters used in it via spatial positioning experiments using a coordinate measuring machine. Based on the parameter identification results, we calibrate this robot-type machine tool and evaluate its machining performance in terms of the dimensional accuracy and contour accuracy of the machined workpiece.

Keywords: parallel mechanism, calibration, forward kinematics, articulated arm coordinate measuring machine (AACMM), robot-type machine tool (RTMT)

Nomenclature

axis 1, 2, 3	Length of one-, two-, and three-axes
axis C, A	Angle of C- and A-axes
φ_i	Angle of joint; approximate solution of nonlinear simultaneous equations
$O_{B,\,M,\,T}$	Coordinate system of base, moving platform, and tool tip coordinate
R	Joint of 1-axis from base
S	Joint of 2-axis from base
T	Joint of 3-axis from base
R', S', T'	Points in X-direction from points R, S, T
S''	Point in Y-direction from point S
P_i	Position vector from O_M to each point
λ_i	Form of base
b_i	Vertical error at base of 1-axis, 2-axis, and 3-axis
f	Offset in X-direction of 2-axis
e	Offset in Y-direction of 2-axis
B_i	Intersection of 1-axis, 2-axis, 3-axis, and moving platform
B_{1X}, B_{1Y}, B_{1Z}	Coordinate of B_1 from O_M
B_{2X}, B_{2Y}, B_{2Z}	Coordinate of B_2 from O_M
B_{3X}, B_{3Y}, B_{3Z}	Coordinate of B_3 from O_M
w_{2y}, w_{2z}	Rotation of vector w_2 in each direction
R_x, R_y	Rotation of vector R_i in each direction
C	Length of perpendicular line of C-axis and A-axis
X_a, Y_a, Z_a	Coordinates from A-axis to O_T
r_T	Theoretical distance of length from one measurement point to another
r_{TP}	Value of r_T when an error is assigned to a single kinematic parameter
r	Measurement distance
$\boldsymbol{J}$	Jacobian matrix
$\boldsymbol{E}_r$	Error array
$\boldsymbol{E}_P$	Correction values of kinematic parameter error

1. Introduction

The parallel mechanism exhibits excellent features such as high rigidity, high accuracy, and high speed compared with industrial robots composed of only serial links. The parallel mechanism, which began with the Stewart platform announced in 1965, has been investigated for applications such as manipulators, handling robots, coordinate measuring machines, and machine tools [1–7]. For machine tools particularly, structural shapes such as hexapods and tripods have been devised, and tripods are the most typical shape used because of their high rigidity owing to the small number of joints [6, 7].

Machine tools that employ a parallel link mechanism have been developed by the following manufacturers: Giddings & Lewis, Hexel Corporation, Ingersoll Milling Machine Company, Okuma Corporation, and JTEKT Corporation. The hexapod-type structure, in which the spindle is mounted on the platform, has become the main-

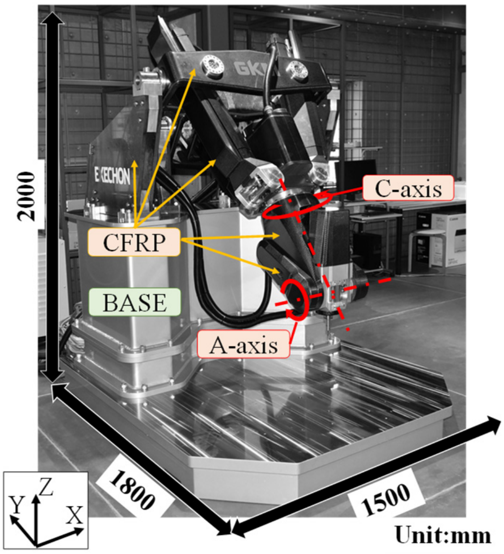

Fig. 1. Appearance and dimensions of XMINI [12].

Table 1. Specifications of XMINI.

Item	Eng. units	Specifications
Maximum rapid traverse speed	m/min	90
Maximum speed of *C*- and *A*-axes	min^{-1}	37
Maximum feed rate	m/min	35
Stroke of 1- to 3-axis (ball screw driving mechanism)	mm	563/864
Rotation *A*-axis (belt driving mechanism without reducer)	degree	−4/115
Rotation *C*-axis (direct driving mechanism)	degree	±360
Least command increment	mm	0.001
Maximum spindle speed	min^{-1}	20000
Spindle power	kW	11.5
Module weight (exclude base)	kg	250
NC controller	–	Simens 840 solution line

stream structure [8].

Meanwhile, tripod-type machine tools are manufactured by Metron, Loxin, and Exechon. This type of machine tool has the same degree of freedom (DOF) as a five-axis machining center, and the spindle is attached to a platform such as a hexapod. Among them, the Exechon robot-type machine tool (RTMT) used in this study exhibits a tripod structure composed of a three-axis telescopic shaft and a moving platform; moreover, by attaching the *C*- and *A*-axes to the platform, the movable range of the tool tip position was successfully widened. Furthermore, Exechon proposed an RTMT with a new parallel mechanism that exhibits a CFRP structure with higher rigidity than other milling machines [9–11]. This machine comprises a parallel mechanism (one- to three-axis) and a serial mechanism (*A*- and *C*-axes), which is a type of five-axis machine tool. A moving platform with the same function as the Stewart platform is mounted on the ends of the three axes to support the *A*- and *C*-axes, as shown in **Fig. 1**, and the specifications are listed in **Table 1**. This machine tool enables a relatively wide, lightweight, and easy to disassemble and/or move working space to be secured. However, when this machine tool is used for machining, estimations of the dimensional errors, assembly errors, tool trajectory, and positioning errors must be solved (hereinafter referred to as calibration). The tool endpoint posture must be compensated based on the estimated kinematic parameters via calibration.

Many studies have focused on the calibration method for kinematics machine tools [13–25]. Forward kinematics problems have been investigated for various types of kinematics machines [26–28].

In a study pertaining to a tripod-type machine tool manufactured by Exechon, Trinh et al. discovered a solution to the forward kinematics problem [11]. In addition, Bi developed a stiffness model based on the Exechon concept [29].

The authors developed a solution for the forward kinematics problem by adopting the proposed calibration method [13, 19]. This method uses an articulated arm coordinate measuring machine (AACMM). It is not necessary to strictly define the position and orientation of the AACMM coordinate to that of the target machine tool. The advantage of this method is that the unknown kinematics parameters can be estimated by measuring the distances between two points and by extracting the machine coordinates from the CNC controller. The measurements are obtained repetitively by the number of unknowns using the distance acquired by the AACMM at different points. In addition, compared with the DBB measurement method, the measurable space was extremely wide, thereby allowing various postures that are acceptable for calibration measurement to be set. Small robot machine tools, such as the RTMT, can be relocated frequently. However, the values of the kinematics parameters will change based on the relocated positions. Therefore, a simple and easy-to-apply calibration operation is required.

Because this RTMT exhibits orthogonal anisotropic rigidity based on the position, many problems related to machining accuracy arise when performing contour machining using this machine tool. Therefore, the RTMT, which is primarily used by installing it on rails or by suspending it on a ceiling as a gantry and rendering it movable in a factory, has been developed primarily for drilling pilot holes on body riveting airplanes. Therefore, in this study, we primarily focused on improving the accuracy of drilling and boring after performing spatial positioning. Improving the performance of contour machining accuracy is another issue to be addressed in this study.

This paper reports the improved positioning accuracy and machining performance of a test workpiece based on a previously proposed calibration method.

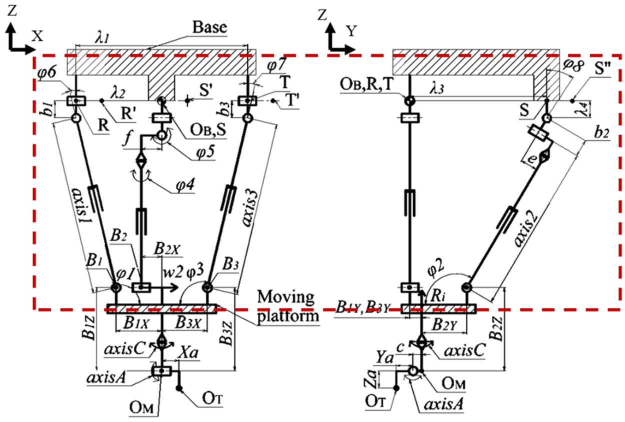

Fig. 2. Skeleton diagram of XMINI (symbols related to the mechanism in the figure are displayed based on JIS B 0138).

2. Identification of Kinematic Parameters by Proposed Calibration Method

2.1. Geometric Arrangement for Forward Kinematics

The results of positioning control and machining performance based on the calibration method are presented in this section.

Figure 2 shows the skeleton diagram of the RTMT, which is a five-axis machine tool that combines a parallel mechanism with three telescopic axes (three degrees of freedom (3-DOFs)), and a pair of serial mechanisms comprising two rotating axes (2-DOFs). The three telescopic axes were positioned by controlling each length unit (*axis1* mm, *axis2* mm, *axis3* mm), and the other two axes were controlled by rotational angle units (*axis-C*°, *axis-A*°). These axes have axis variables φ_1, φ_2, φ_3, φ_4, φ_5, φ_6, φ_7, and φ_8, which are expressed by nonlinear simultaneous equations using angular units "degree." These are included in the position vector, as is shown later. O_B, O_M, and O_T are the coordinates of the base, moving platform, and tool tip, respectively.

The positions of each coordinate system are shown in **Fig. 2**. The joint points of each axis and base are R, S, and T, respectively. Points R', T', and S' are points in the X-direction from points R, T, and S, respectively, and S'' is point S in the Y-direction. The position vectors from O_M to points R, S, T, R', S', S'', and T' are denoted as $\boldsymbol{P}_R$, $\boldsymbol{P}_S$, $\boldsymbol{P}_T$, $\boldsymbol{P}_{R'}$, $\boldsymbol{P}_{S'}$, $\boldsymbol{P}_{S''}$, and $\boldsymbol{P}_{T'}$, respectively. It is noteworthy that subscripts X, Y, and Z, such as those in the expression of P_{RX}, represent the position vector components [13, 19].

2.2. Obtained Kinematics Parameters Correction Value

The data acquired to calculate the kinematics parameters were the distances between representative points. The relationship between the minute displacement δr_T of the theoretical value r_T and the sum of the minute displacement δP of the kinematic parameter P is expressed as follows using m (the m_{th} number of r and r_T) and n (the n_{th} number of the kinematics parameters). Here, r_T is the square root of the sum of the squared differences between the coordinates of the two measured points.

$$\delta r_{Tm} = \frac{\Delta r_{Tm}}{\Delta P_1}\delta P_1 + \frac{\Delta r_{Tm}}{\Delta P_2}\delta P_2 + \cdots + \frac{\Delta r_{Tm}}{\Delta P_n}\delta P_n \quad . \quad (1)$$

Assuming that the minute displacement δr_T of the theoretical value r_T is replaced by the difference between the measured value r and the theoretical value r_T, Eq. (1) can be rewritten as follows:

$$r_m - r_{Tm} = \frac{\Delta r_{Tm}}{\Delta P_1}\delta P_1 + \frac{\Delta r_{Tm}}{\Delta P_2}\delta P_2 + \cdots + \frac{\Delta r_{Tm}}{\Delta P_n}\delta P_n \quad (2)$$

It is difficult to obtain the total derivative r_T because r_T contains the solution of the nonlinear simultaneous equations, and the kinematic parameters are included in the constraints; φ_i is a variable of the kinematic parameters. However, in the forward kinematics problem, the numerical value of the approximated φ_i can be substituted. Therefore, φ_i cannot be partially differentiated using kinematics parameters. To solve this problem, assuming that r_T is defined as r_{TP} when an arbitrary error is assigned only to variable P_n, Eq. (2) can be transformed as shown in the following equation.

$$\frac{\Delta r_{Tm}}{\Delta P_n} = \frac{r_{TPmn} - r_{Tm}}{\delta P_n} \quad . \quad (3)$$

Hence, the Jacobian matrix $\boldsymbol{J}$ is transformed as follows:

$$\boldsymbol{J} = \begin{pmatrix} \dfrac{r_{TP11} - r_{T1}}{\delta P_1} & \cdots & \dfrac{r_{TP1n} - r_{T1}}{\delta P_n} \\ \vdots & \ddots & \vdots \\ \dfrac{r_{TPm1} - r_{Tm}}{\delta P_1} & \cdots & \dfrac{r_{TPmn} - r_{Tm}}{\delta P_n} \end{pmatrix} \quad . \quad (4)$$

Deriving the difference between r_T and r, the array $\boldsymbol{E}_r$ is defined as shown in the following equation:

$$\boldsymbol{E}_r = [\boldsymbol{r}_1 - \boldsymbol{r}_{T1} \quad \boldsymbol{r}_2 - \boldsymbol{r}_{T2} \quad \ldots \quad \boldsymbol{r}_m - \boldsymbol{r}_{Tm}]^T \quad . \quad (5)$$

Next, the correction value $\boldsymbol{E}_P$ of the kinematics parameters is calculated using the following equation:

$$\boldsymbol{E}_P = \left(\boldsymbol{J}^T \boldsymbol{J}\right)^{-1} \boldsymbol{J}^T \boldsymbol{E}_r \quad . \quad (6)$$

As a result of the correction, the calculation is terminated when $\boldsymbol{E}_r$ is within the required accuracy. Otherwise, the least-squares calculation is repeated using the modified $\boldsymbol{E}_r$ until it converges to a certain value (target tolerance: 5e-07 μm).

3. Parameter Identification Results

A total of 26 kinematics parameters are shown in **Fig. 2**. Because of redundancy, 23 kinematics parameters are to be identified. Therefore, some kinematics parameters were omitted or integrated. Because λ_3 and λ_4 are completely redundant, λ_4 is omitted. Additionally, B_{1Y} and B_{3Y} are redundant because B_{1Y} and B_{3Y} have the same

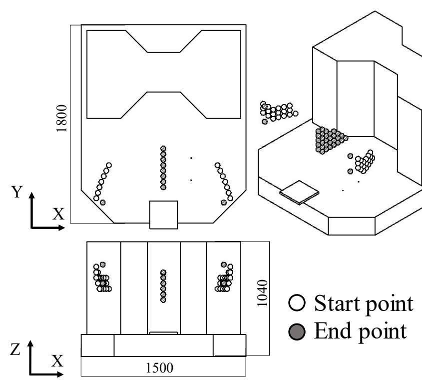

Fig. 3. Position layout of distance measurements.

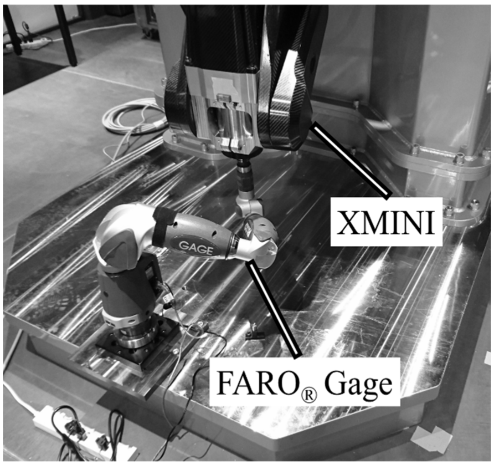

Fig. 4. Experimental setup for measuring distance using coordinate measuring machine.

Table 2. Specifications of FARO® Gage.

Name	Unit	Specification
Accuracy	mm	0.018
Spherical working volume	m	1.2
Can be measured	–	Position, posture*

*Do not use posture

Table 3. Calculation result.

	Number of least-squares runs			
	1st	2nd	3rd	4th
λ_1 mm	0.505	0.500	0.500	0.500
λ_2 mm	1.062	1.060	1.060	1.060
λ_3 mm	0.622	0.638	0.640	0.638
λ_4 mm	Redundant parameter			
b_1 mm	0.108	0.189	0.195	0.191
b_2 mm	−0.452	−0.385	−0.379	−0.384
b_3 mm	−0.061	0.006	0.010	0.007
f mm	0.592	0.736	0.817	0.773
e mm	1.040	1.022	1.020	1.020
B_{1X} mm	−0.029	−0.019	−0.018	−0.018
B_{1Y} mm and B_{3Y} mm	−0.757	−0.738	−0.741	−0.739
B_{1Z} mm and B_{3Z} mm	0.444	0.436	0.436	0.435
B_{2X} mm	−0.545	−0.652	−0.723	−0.686
B_{2Y} mm	0.549	0.557	0.557	0.557
B_{2Z} mm	0.746	0.735	0.735	0.734
B_{3X} mm	0.411	0.423	0.423	0.423
$w2y$°	−0.033	−0.033	−0.033	−0.033
$w2z$°	0.029	0.034	0.036	0.035
Rx°	−0.122	−0.120	−0.120	−0.120
Ry°	−0.021	−0.021	−0.021	−0.021
c mm	−0.071	−0.069	−0.069	−0.069
X_a mm	−0.090	−0.088	−0.087	−0.087
Y_a mm	0.147	0.147	0.147	0.147
Z_a mm	−1.534	−1.533	−1.533	−1.533

length.

It was previously reported that the measurement points should be arranged in a wide three-dimensional space [10, 11]. Therefore, the measurement points were placed as far from each other as possible within the movable range of the RTMT.

The measurement points were set such that the mechanical parameters were not redundant. Two points were sequentially extracted from the measurement points acquired in this manner, and the distance between each point was calculated. The measurement points are shown in **Fig. 3**. The number of measurement points was 102, and the number of distances r to be acquired from these points was 2432.

In this experiment, the AACMM (FARO® Gage), as shown in **Fig. 4** and **Table 2** (specifications), was used by attaching the base plate and end of the A-axis of the RTMT. The room temperature was set to 20°C [22], and the experiments were conducted twice. The coordinates were acquired by positioning the RTMT at each measurement point. The AACMM settings and coordinate acquisition were based on the xCAL software provided by Exechon Enterprises LLC.

When r_T was acquired beyond the center shown in **Fig. 4**, kinematic parameters with reversed error signs were obtained, and the error was canceled out; hence, a valid r_T could not be obtained, such as the kinematic parameter f. **Table 3** shows the results of 23 parameters. In addition, **Fig. 5** shows the deviation between the identified value and the factory initial setting values. The horizontal axis shows the kinematics parameters, and the vertical axis shows the calculated values. The value of the actual component $\boldsymbol{E}_r$ was not always within ±0.5 μm. Therefore, the calculation was terminated when $\boldsymbol{E}_r$ stabilized. Least-squares trials were executed four times.

4. Machining Test and its Evaluation

In this study, a machining accuracy evaluation test was conducted based on ISO 10791-7:2020 (JIS B 6336-7), "Accuracy of Finished Test Pieces" [30]. **Table 4** presents an outline of the machining test. **Fig. 6(a)** shows the shape and data of the test piece. The specimen setting at the base

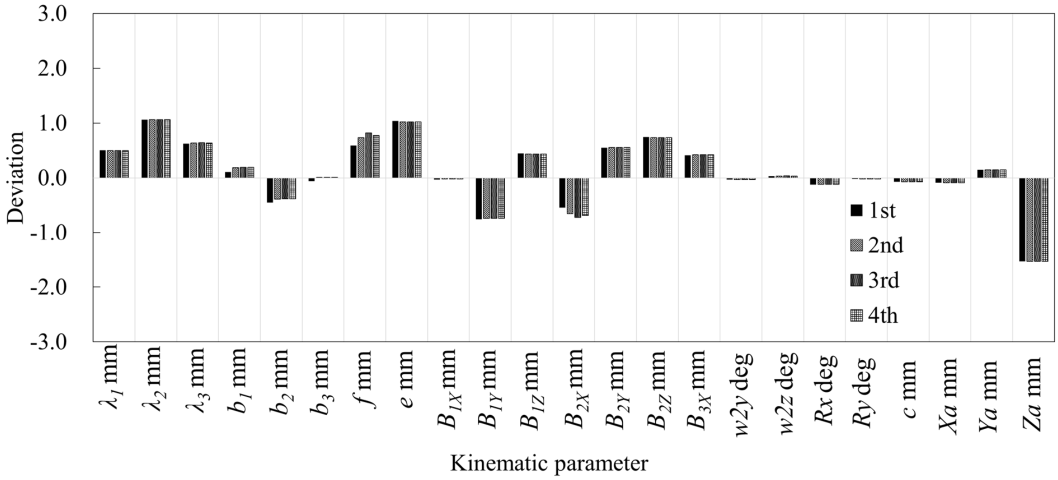

Fig. 5. Error fluctuation of kinematics parameters in each measurement.

Table 4. Machining conditions.

Item		Eng. units	Specifications
Test piece			ISO 10791-7:2020
Material		–	(AlCu4MgSi (A), A2017AP)
End mill	Tool diameter	mm	13/30
ϕ3	Teeth	–	2
HSK-A40	Helix angle	degree	40
-HDC10-75	Tool protrusion length	mm	32/70
ϕ30	Cutting speed	m/min	84.8
HSK-A40	Feed	mm/tooth	0.05
-CT25SA-105	Radial depth of cut	mm	0.2
	Tool diameter	mm	26
Boring tool	Tooth	–	1
HSK-A40	Tool protrusion length	mm	78
-CX81-78	Cutting speed	m/min	42.4
	Feed	mm/tooth	0.01
	Radial depth of cut	mm/tooth	0.1
Cutting direction			Down-cut
Tool interface			HSK-E40
Room temperature		°C (K)	20 (293)

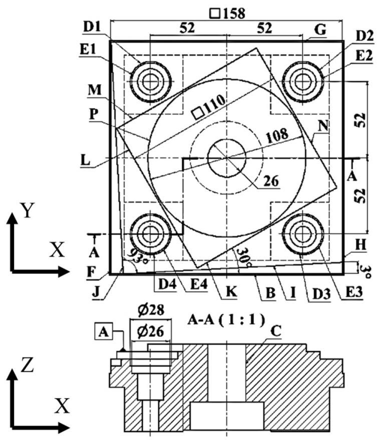

(a) Workpiece drawing of ISO 10791-7:2020 [30]

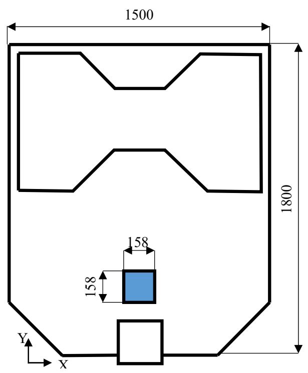

(b) Machined area of workpiece

Fig. 6. Target workpiece and its set place.

of the RTMT is shown in **Fig. 6(b)**. Regarding the shape of the workpiece, the outer diameter was changed from 160 to 158 mm owing to the limited movable range of the RTMT.

Although the tool in the upward/downward direction can be positioned based on the *A*- and *C*-axes, the tool direction was set in the downward direction in this study. Therefore, the problems caused by the dynamic behavior of the *A*- and *C*-axes were negligible.

The workpiece was fabricated using an aluminum alloy (A2017AP, AlCu4MgSi (A)). The tool used was a square-type ϕ30 mm end mill. A center hole was drilled in advance using a ϕ25 mm twist drill and then finished to ϕ26 mm using the boring tool.

The other holes were spirally machined with a ϕ13 mm diameter two-flute square end mill. The cutting speed was slower than the ISO recommended value; however, it was determined by considering the machined surface properties of the workpiece obtained during the preliminary experiment. In particular, the machining conditions were set such that chatter vibrations did not occur during workpiece contouring from prior experiments.

Regarding the end mill, the feed rate per tooth was set

Table 5. Measured geometric tolerance.

No.	Geometric tolerance	Initial setting	1st calibrate	2nd calibrate
1	Cylindricity of data form *C* (borehole)	0.039	0.043	0.046
2	The perpendicularity of the center line of datum feature *C* (borehole) to data plane *A*	0.030	0.079	0.108
3	Straightness of side *B*	0.028	0.072	0.057
4	Straightness of side *F*	0.010	0.008	0.010
5	Straightness of side *G*	0.019	0.029	0.101
6	Straightness of side *H*	0.006	0.010	0.009
7	Right angle of side *H* to datum plane *B*	0.469	0.092	0.137
8	Squareness of side *F* with respect to datum plane *B*	0.437	0.112	0.132
9	Parallelism of side *G* with datum plane *B*	0.121	0.148	0.169
10	Straightness of side *K*	0.067	0.076	0.070
11	Straightness of side *L*	0.053	0.047	0.049
12	Straightness of side *M*	0.077	0.088	0.079
13	Straightness of side *N*	0.039	0.053	0.034
14	30° slope of side *K* with respect to datum plane *B*	0.069	0.084	0.124
15	60° slope of side *L* with respect to datum plane *B*	0.266	0.066	0.110
16	30° slope of side *M* with respect to datum plane *B*	0.082	0.094	0.134
17	60° slope of side *N* with respect to datum plane *B*	0.276	0.118	0.092
18	Roundness of contoured circle *P*	0.275	0.122	0.086
19	Concentricity between datum feature *C* (borehole) and outer circle *P*	0.274	0.422	0.227
20	Straightness of side *I*	0.072	0.086	0.065
21	Straightness of side *J*	0.010	0.012	0.018
22	3° slope of side *I* with respect to datum plane *B*	0.120	0.079	0.147
23	93° slope of side *J* with respect to datum plane *B*	0.423	0.095	0.117
24	Position of hole D1 with respect to datum axis straight line *C*	0.321	0.052	0.112
25	Position of hole D2 with respect to datum axis straight line *C*	0.374	0.084	0.243
26	Position of hole D3 with respect to datum axis straight line *C*	0.225	0.104	0.338
27	Position of hole D4 with respect to datum axis straight line *C*	0.357	0.085	0.258
28	Concentricity between outer hole D1 and inner hole E1	0.061	0.055	0.130
29	Concentricity between outer hole D1 and inner hole E2	0.066	0.097	0.045
30	Concentricity between outer hole D1 and inner hole E3	0.082	0.121	0.064
31	Concentricity between outer hole D1 and inner hole E4	0.055	0.052	0.087

to $1/5$ that of the end mill in accordance with the ISO standard. The radial depth of cut for finish cutting was determined in accordance with ISO recommended conditions for end mills, and the feed of the boring bite was set to half that of end mills. In addition, all machining directions were reduced.

A coordinate measuring machine (CRYSTA-APEX-9109, manufactured by Mitutoyo) was used to measure the geometrical tolerance. The results are presented in **Table 5** and **Fig. 7**. In the table and figure, the initial setting denotes the machined result using the factory default parameters, while the first calibration denotes the machined result using the parameters from the first calculation, and the second calibration shows the machined result using the parameters from the second calculation. These two calibration calculations were independent of each other and not recalculated using the previous results. Hence, the processing result could not be improved, and the results obtained were independent; therefore, the results might deteriorate at the second time.

As shown in **Fig. 7**, the machining accuracy of the workpiece was improved by calibrating, particularly its squareness, inclination, and roundness. Furthermore, it can be concluded that the proposed method is sufficiently effective and appropriate to compensate for the machining performance. This implies that the calibration resulted in an improvement in the motion of the RTMT. However, the positioning accuracy was not as high as expected because some of the positions were worse than the initial position values.

The hole center coordinates were measured and compared with the initial and calibrated settings, as shown in **Figs. 8–11**. When the initial value of the factory default settings was used, the coordinates deviated significantly from the target value occasionally. By contrast, the result of the first calibration was similar to the target value, as

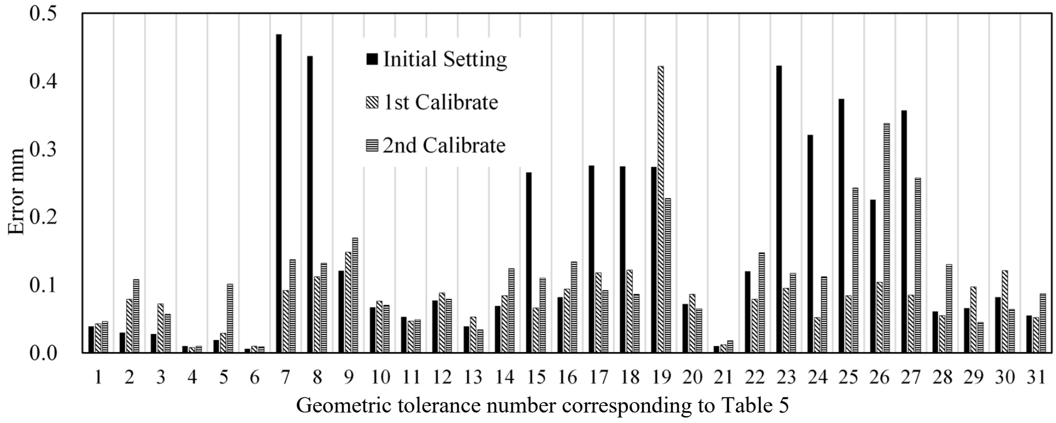

Fig. 7. Measured workpiece deviations at each machining.

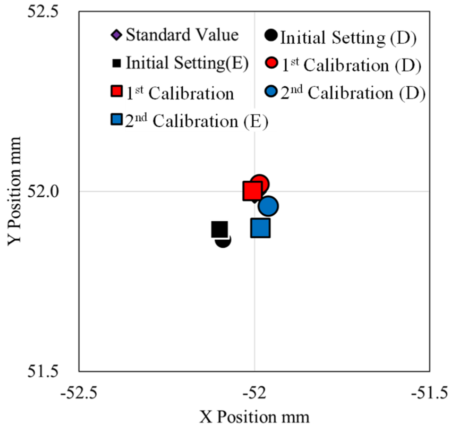

Fig. 8. Position of hole centers D1 and E1.

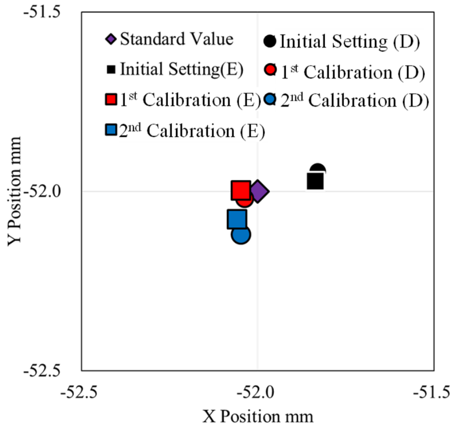

Fig. 10. Position of hole centers D4 and E4.

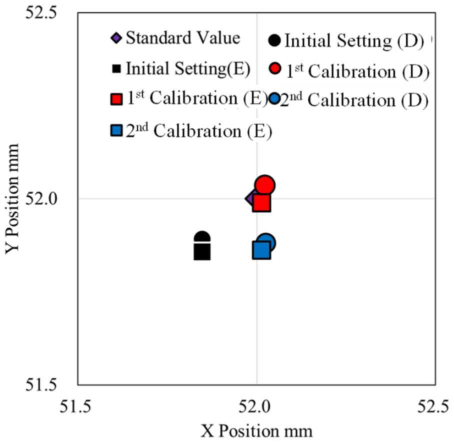

Fig. 9. Position of hole centers D2 and E2.

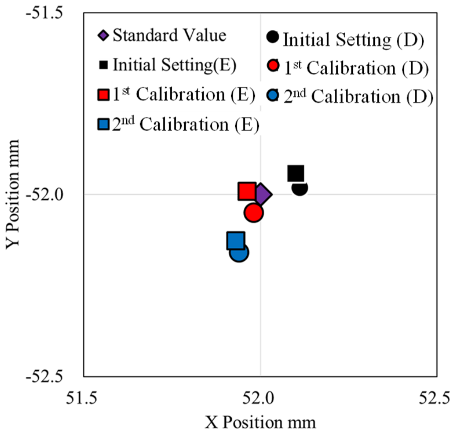

Fig. 11. Position of hole centers D3 and E3.

shown by the measurement results of the distance between the holes in **Table 6**. However, in the second calibration, the positions of the holes in D2, E2, D3, and E3 did not improve as expected.

Figure 12 shows the results for the machined test pieces. By setting the machining conditions moderately in advance, the machined workpiece did not exhibit chatter vibrations on the machined surface. As mentioned previously, this RTMT is more suitable for drilling and boring than contour machining.

The results confirmed that the machining results based on the proposed kinematics parameter calibration are sufficiently effective in improving the machining accuracy because the motion accuracy improved. Although the im-

Table 6. Hole pitches of D1–D4.

	Initial setting		1st calibration		2nd calibration	
	Distance	Error	Distance	Error	Distance	Error
D1–D2	103.937	−0.063	104.008	0.008	103.986	−0.014
D2–D3	103.872	−0.128	104.085	0.085	104.039	0.039
D3–D4	103.941	−0.059	104.018	0.018	103.987	−0.013
D4–D1	103.811	−0.189	104.042	0.042	104.080	0.080

Fig. 12. Machined results.

Table 7. Hole pitches of E1–E4.

	Initial setting		1st calibration		2nd calibration	
	Distance	Error	Distance	Error	Distance	Error
E1–E2	103.946	−0.054	104.200	0.200	103.997	−0.003
E2–E3	103.800	−0.200	103.979	−0.021	103.988	−0.012
E3–E4	103.937	−0.063	104.010	0.010	103.990	−0.010
E4–E1	103.867	−0.133	103.999	−0.001	103.977	−0.023

provement in the accuracy of the RTMT operation and the reproducibility of the mechanical parameter calculation results by calibration did not match at all times, the results shown in **Table 7** were sufficiently good, as in the first calibration; in particular, although the abovementioned estimation results of the kinematics parameters show that b_1, b_2, b_3, f, e, B_{1Y}, B_{2X}, B_{2Z}, and w_{2Z} differed significantly for each trial, these kinematics parameters contributed only slightly to the motion accuracy. They did not impose a single effect, but a combined effect. It was presumed that the low reproducibility of the parameter calculation results was due to the abovementioned slight effect on the measured value. Additionally, the accuracy of the coordinate measuring machine might affect the results.

5. Conclusions

Machining performance in terms of contouring accuracy and positioning accuracy was described based on a calibration method using an AACMM for an Exechon RTMT. The aluminum alloy was machined according to ISO 10791-7:2020. Furthermore, its validity and effectiveness were confirmed through an evaluation based on actual machining. This method demonstrated that the machining accuracy in the X-Y plane (with the Z-axis constant) of the workspace coordinates was sufficiently effective. Nonetheless, the measurement uncertainty based on some methods remains to be evaluated. The spatial accuracy for all movable ranges should be evaluated in the future. Based on these results, further studies are necessitated to investigate the machining of 3D surfaces and the contouring ability of the RTMT.

Acknowledgements

We acknowledge the support provided in terms of equipment provision and equipment operation from Exechon Enterprises LLC, Giken Co., Ltd., and BBS Kinmei Co., Ltd.

References:

[1] T. Harada and K. Dong, "Mechanical Design and Control of 3-DOF Active Scanning Probe Using Parallel Link Mechanism," Int. J. Automation Technol., Vol.5, No.2, pp. 86-90, doi: 10.20965/ijat.2011.p0086, 2011.

[2] G. Ma, Y. Chen, Y. Yao, and J. Gao, "Kinematics and Singularity Analysis of a Four-Degree-of-Freedom Serial-Parallel Hybrid Manipulator," J. Robot. Mechatron., Vol.29, No.3, pp. 520-527, doi: 10.20965/jrm.2017.p0520, 2017.

[3] S. Sakakibara, "Genkotsu-Robot and its Application Systems," J. of the Robotics Society of Japan, Vol.30, No.2, pp. 154-156, doi: 10.7210/jrsj.30.154, 2012 (in Japanese).

[4] Y. Takeda, "Kinematic Structure and Characteristics of Parallel Manipulators" The Robotics Society of Japan, Vol.30, No.2, pp. 124-129, doi: 10.7210/jrsj.30.124, 2012 (in Japanese).

[5] T. Oiwa, "Precision Mechanism Based on Parallel Kinematics," Int. J. Automation Technol., Vol.4, No.4, pp. 326-337, doi: 10.20965/ijat.2010.p0326, 2010.

[6] J.-S. Chen, "Design and analysis of a tripod machine tool with an integrated Cartesian guiding and metrology mechanism," Vol.28, Issue 1, pp. 46-57, doi: 10.1016/S0141-6359(03)00073-4, 2004.

[7] F. Gao, "A novel 5-DOF fully parallel kinematic machine tool," The Int. J. of Advanced Manufacturing Technology, Vol.31, pp. 201-207, doi: 10.1007/s00170-005-0171-1, 2006.

[8] T. Shibukawa, T. Toyama, and K. Hattori, "Parallel Mechanism Based Milling Machine," J. of JSPE, Vol.63, No.12, pp. 1671-1675, doi: 10.2493/jjspe.63.1671, 1997.

[9] K. Neumann, "The key to aerospace automation," Proc. of the SAE Aerospace Manufacturing and Automated Fastening Conf. and Exhibition, 2006-01-3144, doi: 10.4271/2006-01-3144, 2006.

[10] K. Neumann, "Practical and Portable Automated Machining," Proc. of the SAE Aerospace Manufacturing and Automated Fastening, 2014-01-2275, doi: 10.4271/2014-01-2275, 2014.

[11] D.-C. Trinh, D. Zlatanov, M. Zoppi, and R. Molfino, "Direct Kinematics of the Exechon Tripod," Proc. of ASME IDETC/CIE, doi: 10.1115/DETC2016-60038, 2016.

[12] http://exechon.com/xmini/ [Accessed April 19, 2021]

[13] K. Nagao, N. Fujiki, Y. Morimoto, and A. Hayashi, "Calibration Method of Parallel Mechanism Type Machine Tools," Int. J. Automation Technol., Vol.14, No.3, pp. 429-437, doi: 10.20965/ijat.2020.p0429, 2020.

[14] S. Aoyagi, M. Suzuki, T. Takahashi, Fujioka, and Y. Kamiya, "Calibration of Kinematic Parameters of Robot Arm Using Laser Tracking System: Compensation for Non-Geometric Errors by Neural Networks and Selection of Optimal Measuring Points by Genetic Algorithm," Int. J. Automation Technol., Vol.6, No.1, pp. 29-37, doi: 10.20965/ijat.2012.p0029, 2012.

[15] H. Yachi and H. Tachiya, "Calibration Method for a Parallel Mechanism Type Machine Tool by Response Surface Methodology – Consideration via Simulation on a Stewart Platform Mechanism –," Int. J. Automation Technol., Vol.4, No.4, pp. 355-363, doi: 10.20965/ijat.2010.p0355, 2010.

[16] H. Ota, T. Shibukawa et al., "Study of Kinematic Calibration Method for Parallel Mechanism (2nd Report) – Kinematic Calibration Using Forward Kinematics –," J. of JSPE, Vol.66, No.10, pp. 1568-1572, doi: 10.2493/jjspe.66.1568, 2000 (in Japanese).

[17] S. Ibaraki, T. Yokawa et al., "A Study on the Improvement of Motion Accuracy of Hexapod-type Parallel Mechanism Machine Tool (2nd Report) – A Calibration Method to Evaluate Positioning Errors on the Global Coordinate System –," J. of JSPE, Vol.70, No.4, pp. 557-561, doi: 10.2493/jspe.70.557, 2004 (in Japanese).

[18] Y. Takeda, G. Shen, and H. Funabashi, "Kinematic Calibration of In-Parallel Actuated Mechanisms Using Fourier Series (1st Report, Calibration Method and Selection Method of the Set of Measurement Paths)," JSME Int J., Series C, Vol.68, No.673, pp. 2762-2769, doi: 10.1299/kikaic.68.2762, 2002 (in Japanese).

[19] K. Nagao, N. Fujiki, and Y. Morimoto, "Study on calibration method of parallel mechanism type machine tools – Solution of forward kinematics problem considering kinematic error –," Proc. of the 2019 Annual Meeting of the JSPE, pp. 217-218, doi: 10.11522/pscjspe.2019S.0_217, 2019.

[20] M. Nakagawa, T. Matsushita et al., "A Study on the Improvement of Motion Accuracy of Hexapod-type Parallel Mechanism Machine Tool (1st Report) – The Method of Kinematic Calibration Without Gravitation Deformation –," J. of JSPE, Vol.67, No.8, doi: 10.2493/jjspe.67.1333, 2001 (in Japanese).

[21] G. Shen, T. Takeda, and H. Funabashi, "Kinematic Calibration of In-Parallel Actuated Mechanisms Using Fourier Series (2nd Report, Experimental Investigations)," JSME Int J., Series C, Vol.69, No.682, pp. 227-234, doi: 10.1299/kikaic.69.1691, 2003 (in Japanese).

[22] O. Sato, K. Shimojima, R. Furutani et al., "Artifact Calibration of Parallel Mechanism (1st Report) – Kinematic Calibration with a Priori Knowledge –," J. of JSPE, Vol.70, No.1, pp. 96-100, doi: 10.2493/jspe.70.96, 2004 (in Japanese).

[23] N. Zimmermann and S. Ibaraki, "Self-calibration of rotary axis and linear axes error motions by an automated on-machine probing test cycle," The Int. J. of Advanced Manufacturing Technology, Vol.107, pp. 2107-2120, doi: 10.1007/s00170-020-05105-3, 2020.

[24] S. Ibaraki, "Kinematic modeling and error sensitivity analysis for on-machine five-axis laser scanning measurement under machine geometric errors and workpiece setup errors," The Int. J. of Advanced Manufacturing Technology, Vol.96, pp. 4051-4062, doi: 10.1007/s00170-018-1874-4, 2018.

[25] S. Ibaraki, T. Yokawa et al., "A Study on the Improvement of Motion Accuracy of Hexapod-type Parallel Mechanism Machine Tool (3rd Report) – A Kinematic Calibration Method Considering Gravity Errors –," J. of JSPE, Vol.72, No.3, pp. 355-359, doi: 10.2493/jspe.72.355, 2004 (in Japanese).

[26] M. Hashimoto and Y. Imamura, "Kinematic Analysis and Design of a 3DOF Parallel Mechanism for a Passive Compliant Wrist of Manipulators," JSME Int J., Series C, Vol.64, Issue 622, pp. 2116-2123, doi: 10.1299/kikaic.64.2116, 1998 (in Japanese).

[27] R. Kang, H. Chanal, T. Bonnemains, S. Pateloup, D. Branson, and P. Ray, "Learning the forward kinematics behavior of a hybrid robot employing artificial neural networks," Robotica, Vol.30. pp. 847-855, doi: 10.1017/S026357471100107X, 2012.

[28] T. Oiwa, M. Kyogoku, and K. Yamaguchi, "Coordinate Measuring Machine using Parallel Mechanism (5th Report) – Kinematic Calibration with Three-Dimensional Ball Plate –," J. of JSPE, Vol.68, No.1, pp. 65-69, doi: 10.2493/jjspe.68.65, 2002 (in Japanese).

[29] Z. Bi, "Kinetostatic modeling of Exechon parallel kinematic machine for stiffness analysis," The Int. J. of Advanced Manufacturing Technology, Vol.71, No.10, pp. 325-335, doi: 10.1007/s00170-013-5482-z, 2014.

[30] JIS B 6336-7:2018 and Int. Organization for Standardization, "10791-7 Accuracy of Finished Test Pieces," 2020.

Name:
Keisuke Nagao

Affiliation:
Kanazawa Institute of Technology

Address:
7-1 Ohgigaoka, Nonoichi, Ishikawa 921-8501, Japan

Brief Biographical History:
2018- Kanazawa Institute of Technology
2019- Graduate School of Engineering, Kanazawa Institute of Technology

Main Works:
• "Study on calibration method of parallel mechanism type machine tools – Solution of forward kinematics problem considering kinematic error –," Proc. of the 2019 Annual Meeting of the JSPE, pp. 217-218, doi: 10.11522/pscjspe.2019S.0_217, 2019.

Membership in Academic Societies:
• Japan Society for Precision Engineering (JSPE)

Name:
Nobuaki Fujiki

Affiliation:
Associate Professor, Kanazawa Institute of Technology

Address:
7-1 Ohgigaoka, Nonoichi, Ishikawa 921-8501, Japan

Brief Biographical History:
1992- Nachi-Fujikoshi Corp.
1999- Assistant, Kanazawa Institute of Technology
2008- Associate Professor, Kanazawa Institute of Technology

Main Works:
• "Bilateral Servo Mechanisms via Adaptive Control," J. of the Japan Society for Precision Engineering, Vol.68, No.6, pp. 806-810, 2002.

Membership in Academic Societies:
• Japan Society of Mechanical Engineers (JSME)
• Robotics Society of Japan (RSJ)

Name:
Hiroto Tanaka

Affiliation:
Graduate Student, Kanazawa Institute of Technology

Address:
7-1 Ohgigaoka, Nonoichi, Ishikawa 921-8501, Japan

Brief Biographical History:
2020 Received Bachelor of Science in Engineering from Kanazawa Institute of Technology

Membership in Academic Societies:
• Japan Society for Precision Engineering (JSPE)

Name:
Akio Hayashi

Affiliation:
Associate Professor, Kanazawa Institute of Technology

Address:
7-1 Ohgigaoka, Nonoichi, Ishikawa 921-8501, Japan

Brief Biographical History:

2014 Received Ph.D. in Engineering from Graduate School of Engineering, Kobe University
2014- Assistant Professor, Kanagawa University
2017- Assistant Professor, Kanazawa Institute of Technology
2021- Associate Professor, Kanazawa Institute of Technology

Main Works:

- "Simulation of Energy Consumption of Machine Tool Motion for 3-Axis Machining," J. of Energy and Power Engineering, Vol.11. pp. 37-43, 2017.
- "Rotational speed control system of water-driven spindle," J. of the Int. Societies for Precision Engineering and Nanotechnology, Vol.51, pp. 88-96, 2017.

Membership in Academic Societies:

- Japan Society of Mechanical Engineers (JSME)
- Japan Society for Precision Engineering (JSPE)

Name:
Hidetaka Yamaoka

Affiliation:
Associate Professor, Mathematics and Science Academic Foundations Programs, Kanazawa Institute of Technology

Address:
7-1 Ohgigaoka, Nonoichi, Ishikawa 921-8501, Japan

Brief Biographical History:

2005 Received Ph.D. from Department of Applied Mathematics and Physics, Graduate Scholl Informatics, Kyoto University
2006- Research Scientist, VCAD System Research Program, The Institute of Physical and Chemical Research (RIKEN)
2012- Lecturer, Kanazawa Institute of Technology
2017- Associate Professor, Kanazawa Institute of Technology

Main Works:

- "Rotational-Vibrational Energy Spectra of Triatomic Molecules Near Relative Equilibria," J. of Mathematical Physics, Vol.49, 043505, 2008.
- "Continuum Dynamics on A Vector Bundle for A Directed Medium," J. of Physics A: Mathematical and Theoretical, Vol.43, 325209, 2010.
- "Practice of Calculus Lecture Using Peer Instruction by Audience Response System," Proc. of the 2020 11th Int. Conf. on E-Education, E-Business, E-Management, and E-Learning (IC4E 2020), pp. 279-283, 2020.

Membership in Academic Societies:

- Mathematical Society of Japan (MSJ)
- Japanese Society for Engineering Education (JSEE)

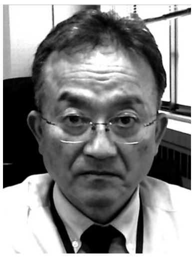

Name:
Yoshitaka Morimoto

Affiliation:
Professor, Kanazawa Institute of Technology

Address:
7-1 Ohgigaoka, Nonoichi, Ishikawa 921-8501, Japan

Brief Biographical History:

1983- Research Worker, Industrial Research Institute of Ishikawa
1996- Associate Professor, Toyama National College of Technology
1999- Associate Professor, Utsunomiya University
2008- Professor, Kanazawa Institute of Technology
2013- Advanced Materials Science Research and Development Center, Kanazawa Institute of Technology
2016- Dean of Academic Affairs, Kanazawa Institute of Technology

Main Works:

- "Vibration Control of Relative Tool-Spindle Displacement for Computer Numerically Controlled Lathe With Pipe Frame Structure," ASME J. of Manufacturing Science and Engineering, Vol.136, No.4, Paper No: MANU-13-1072, doi: 10.1115/1.4027594, 2012.
- "Development of Cutting Device with Enlargement Mechanism of Displacement – Application of Non-Circle Cutting –," J. of Advanced Mechanical Design, Systems, and Manufacturing, Vol.2, No.4, pp. 474-481, 2008.

Membership in Academic Societies:

- American Society of Mechanical Engineers (ASME)
- Japan Society of Mechanical Engineers (JSME), Fellow
- Japan Society for Precision Engineering (JSPE)